HEFAT 2010
7th International Conference on Heat Transfer, Fluid Mechanics and Thermodynamics
Antalya, Turkey, 19-21 Jul 2010

PARAMETRIC INVESTIGATION OF A SYNTHETIC JET HEAT SINK FOR ENHANCED MICRO-SCALE HEAT TRANSFER

T T Chandratilleke*, D Jagannatha and R Narayanaswamy
*Author for correspondence
Department of Mechanical Engineering
Curtin University of Technology
GPO Box U 1987, Perth
Western Australia
Email: t.chandratilleke@curtin.edu.au

ABSTRACT

This paper examines the characteristics of a pulsating fluid jet known as synthetic jet and its cooling effectiveness for heated micro fluid passages. The jet mechanism uses an oscillating diaphragm to inject a high-frequency fluid jet with a zero net mass flow through the jet orifice. The pulsed jet and the micro passage flow interaction is modelled as a 2-dimensional finite volume simulation with unsteady Reynolds-averaged Navier-Stokes equations. For a range of conditions, the special characteristics of this periodically interrupted flow are identified while predicting the associated convective heat transfer rates. The results indicate that the pulsating jet leads to outstanding thermal performance in the micro passage increasing its heat dissipation by about 4.3 times compared to a micro passage without jet interaction within the tested parametric range. The degree of enhancement is first seen to grow gently and then rather rapidly beyond a certain flow condition to reach a steady value. The study also identifies the operational limits imposed by the fluid compressibility on the heat transfer characteristics. The proposed strategy has the unique intrinsic ability to generate outstanding degree of thermal enhancement in a micro passage without increasing its flow pressure drop. The technique is envisaged to have application potential in miniature electronic devices where localised cooling is desired over a base heat dissipation load.

NOMENCLATURE

A	Diaphragm amplitude, mm
d_c	Cavity width, mm
d_o	Orifice width, mm
D	channel width, mm
f	diaphragm frequency, kHz
h	Local convective heat transfer coefficient, W/m^2K
h_c	Cavity height, mm
h_o	Orifice height, mm
H	Channel height, mm
L	Heater width, mm
k	Thermal conductivity of air, W/m·K
L_s	Stroke length, m
Nu	Local Nusselt number based on heater length, (hL/k)
Re_c	Reynolds number, $(U_c d_o/\nu)$
S	Stokes Number, $(\sqrt{\omega d_o^2/\nu})$
t	Time, s
T	Time period, (1/f), s
T_b	Bulk temperature, K
T_w	Wall temperature, K
U_c	Characteristic velocity, m/s
u_o	Velocity through orifice, m/s
V_i	Micro passage inlet velocity, m/s

INTRODUCTION

Effective cooling solutions are critical for the design of electronic devices for preventing thermal breakdown and extending working life of semiconductor components. A dramatic increase in internal heat generation in modern microelectronic devices has exacerbated the cooling requirements in recent years. In the face of this, the conventional cooling methods are rapidly becoming inadequate for dissipating intense heat loads often encountered in new microprocessors. The microelectronic industry signals an urgent need to develop practical and effective cooling methods that surpass current thresholds of thermal performance. Microchannel heat sinks have become the frontier technology in this respect and show well recognised potential for meeting high heat dissipation needs.

A review undertaken by Palm [1] estimates that the use of microchannel heat sinks will increase by 10 fold within the next 5 years in view of its high cooling potential achievable. Exponential growth in applications over the past decade has motivated and intensified research to discover novel techniques to further enhance heat transfer capabilities of microchannels towards meeting future demands.

Microchannel behaviour is relatively well understood through established numerical modelling methods and experimentation. Conducting numerical and experimental studies with rectangular microchannels up to 534 μm in size, Lee et al. [2] have shown that the conventional Navier-Stokes equations do accurately predict microchannel characteristics with just 5 percent deviation between numerical and experimental data. Among many others, Qu and Mudawar [3] have also drawn similar conclusions on the use of conventional equations for microchannel analysis. Lee and Garimella [4] have examined the effects of microchannel channel aspect ratio in thermally developing laminar flow. Using a three dimensional numerical model, they developed a generalised correlation for both local and average Nusselt number in terms of microchannel aspect ratio. Having validated against the experimental data for both mini and micro scale ducts, this correlation is universally recognised for its applicability. The present work adopts a conjugate heat transfer model for microchannel analysis in line with the

current state of numerical modelling such as the simulation work by Fedorov and Viskanta [5].

The primary focus of microchannel research is to predict and validate thermal performance. Much less attention has been directed for developing effective thermal enhancement strategies for micro-scale channels. Reviewing published literature on single-phase micro and minichannel heat transfer, Steinke and Kandlikar [6] have cited that the use of internal fins in microchannels is a very promising passive enhancement option although the increased pressure drop would be a design concern. Narayanaswamy et al. [7] report a comprehensive treatment on such internal fins and possibilities for thermal optimisation.

While passive enhancement techniques have conceivable application potential, active methods may prove to be more effective and relevant for future cooling needs, especially if the thermal enhancement is possible without incurring a penalty through increased pressure drop. As discussed in the sections below, the microchannel flow interrupted by a pulsating fluid jet is envisaged to be an option of this nature.

The present study proposes a new active enhancement method for micro fluid passages. It incorporates a pulsating jet arrangement called a "synthetic jet" that interacts with the flow through the micro passages, as shown in Figure 1.

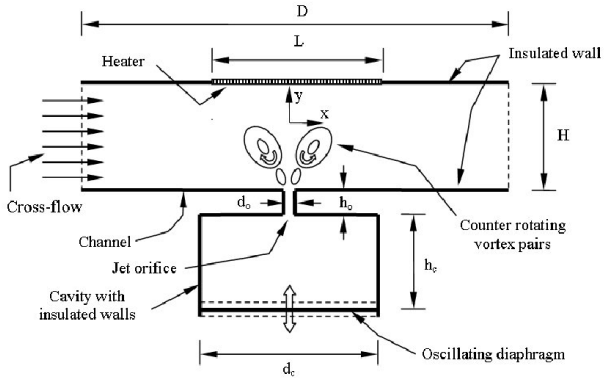

Figure 1. Schematic diagram of synthetic jet mounted on micro fluid passage

The synthetic jet mechanism mounted on the micro passage comprises an oscillating diaphragm that moves back and forth at frequency "f" forcing fluid flow through a small orifice. In its inward motion, the diaphragm imparts a high-speed jet into the micro passage creating a pair of counter-rotating vortices in the surrounding fluid. When retreating, it draws fluid back into the cavity. The fluid ejected through the orifice and the vortices periodically interrupt and interact in cross flow manner with the microchannel fluid flow. Over one diaphragm cycle, the jet discharges an intense net outflow of fluid momentum in to the microchannel while the net mass delivered through the orifice is zero. Therefore, this jet mechanism is known as a "synthetic jet" or Zero-Net-Mass-Flux jet.

In recent years, synthetic jets have been studied in the context of pulsating jet actuators that remove heat from submerged surfaces in quiescent fluid media. Such studies indicate outstanding thermal characteristics for localised cooling with synthetic jets. For example, Campbell et al. [8] have demonstrated that synthetic air micro jets were effective cooling arrangements for laptop processors while Mahalingam et al. [9][10] have developed an integrated active heat sink based on synthetic jets for high power electronic cooling.

The present study proposes to combine the highly favourable characteristics of synthetic jet and the flow through micro passages for developing a novel thermal enhancement strategy for micro-scale heat transfer applications. This hybrid arrangement is envisaged to deliver excellent thermal enhancement for micro passages without requiring large fluid velocities that invariably cause impractical pressure drops.

The vortex formation in synthetic jet occurs under a special parametric condition. Holman et al. [11] showed that the formation is governed by the non-dimensional groups Reynolds number (Re) and Stokes number (S), and is given by $Re/S^2>K$, where the constant $K \approx 1$ for two-dimensional jets and 0.16 for axi-symmetric synthetic jets. This requirement has been duly considered in determining the suitable dimensions for the proposed simulation model.

NUMERICAL MODEL

Solution Domain and Boundary Conditions

Similar to Fugal [12] and Wang [13], the present study uses a numerical model developed on the computational fluid dynamics software FLUENT. A structured mesh was developed for the solution domain shown in Figure 2 using the mesh generation facility GAMBIT. In capturing intricate details of the jet formation and flow separation, the grid density in the vicinity of the orifice was refined to have 14 grid cells in the axial direction and 20 in the transverse direction.

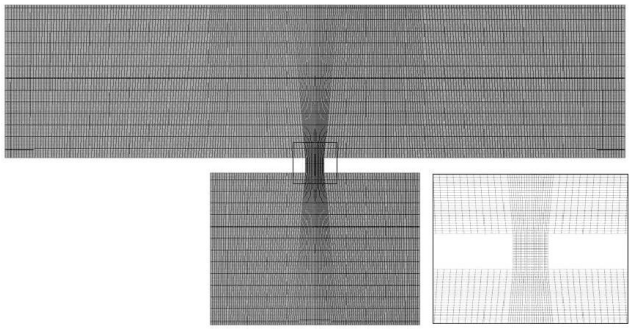

Figure 2. Computational grid for solution domain [Inset shows enlarged view of the marked region]

Appropriate magnitudes of the geometrical dimensions were obtained by considering the synthetic jet formation requirement of $Re/S^2>1$, as shown by Holman et al. [11]. Thus, the following dimensions were used in the analysis: orifice width d_o = 50 μm, orifice length h_o = 50 μm, channel height H = 500 μm, channel length D = 2250 μm, heater length L = 750 μm, cavity width d_c = 750 μm and cavity height h_c = 500 μm. This dimensional selection was checked and confirmed for its compliance with the continuum mechanics for the scale of the attempted problem using Knudsen number Kn, which is the ratio of the molecular free path length to representative length.

The adiabatic conditions were applied at all microchannel walls, the cavity walls and the diaphragm. The heater surface was maintained at an isothermal temperature of 360 K. The (left) flow inlet to the microchannel was treated as a known constant velocity boundary while the (right) flow outlet was taken to be constant static pressure boundary. It was assumed that the working fluid air is incompressible and has an inlet temperature of 300 K with constant thermodynamic properties under standard atmospheric conditions.

Details of the governing equations used and validation of the numerical model can be found in Chandratilleke et al.[14].

Initial Conditions and Solution Methodology

The initial (t = 0) position of the diaphragm was taken to be at the bottom of the cavity. A special User Defined Function (UDF) incorporating Dynamic-layering technique [15] was formulated and combined with the FLUENT solver to describe the periodic diaphragm movement. For this, the diaphragm displacement was expressed as y = A sin (ωt), where A is the diaphragm amplitude, ω is the angular frequency and t is time.

A segregated solution method with implicit solver formulation in FLUENT was used as the numerical algorithm while the Second-order discretisation schemes were employed for density, momentum, pressure, kinetic energy, specific dissipation rate and energy. The Pressure-Implicit with Splitting of Operators (PISO) scheme was used for pressure-velocity coupling. The bulk temperature of air at every time step was calculated using an UDF while the updated bulk temperature was fed back to the simulation for calculating local heat transfer coefficient and Nusselt number.

The jet Reynolds number was calculated based on the jet characteristic velocity U_c, which is defined by Smith [16] as,

$$U_c = L_s f = \frac{1}{T}\int_0^{T/2} u_0(t)\,dt \qquad (1)$$

where $u_o(t)$ is the jet velocity at the orifice discharge plane, ½T is the jet discharge time or half period of diaphragm motion, and L_s is the stroke length (defined as the discharged fluid length through orifice during the upward diaphragm stroke).

With these imposed conditions, the unsteady, Reynolds-averaged Navier-Stokes equations within the solution domain were solved along with the energy equation for a range of operating conditions, which are given in Table 1.

Table 1. Parametric range for the study

Parameter	Range
Micro passage inlet velocity, V_i (m/s)	0, 0.5, 1.0, 2.0
Diaphragm frequency, f (kHz)	10
Diaphragm Amplitude, A (μm)	0, 25, 50, 75, 100
Jet Reynolds Number, Re	15, 30, 46, 62
Orifice to Plate distance, H/d_o	10

The simulation was carried out using 720 time steps per cycle wherein 20 sub-iterations were performed within each time step. At each time step, the internal iterations were continued until the mass, momentum and energy residuals reduced below 10^{-6}, which is the convergence criterion consistently applied for the computation. Data were extracted at every twentieth time step giving 36 data points per cycle. It was observed that 10 diaphragm cycles would be sufficient to achieve quasi-steady conditions in this microchannel flow geometry.

The grid dependency of results was tested by observing the changes to time-averaged velocity fields in the solution domain for varied grid sizes. In view of the moving mesh integrity and CPU time, the most appropriate grid size was found to be 48072 cells for a five percent tolerance between successive grid selections.

RESULTS AND DISCUSSION

Velocity characteristics

Figure 3 illustrates the variation of average jet axial velocity at the orifice and the corresponding diaphragm displacement with time over one complete cycle for an operating frequency of 10 kHz. The jet velocity fluctuation resembling a sinusoidal pattern clearly indicates zero net discharge of fluid mass through the orifice, as anticipated in synthetic jet operation.

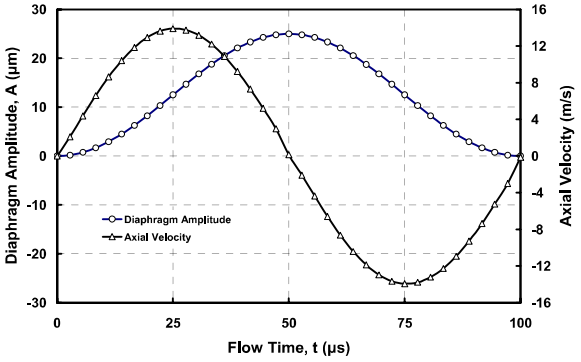

Figure 3. Diaphragm displacement and jet velocity over one complete cycle
at A = 25 μm and f = 10 kHz

Effect of micro passage inlet velocity

Figures 4 (a) and 4 (b) show typical time-lapsed velocity contours within the solution domain respectively for two separate cases of synthetic jet interacting with stagnant fluid as well as flowing fluid in the micro passage.

During the diaphragm upward motion, a high-velocity fluid jet is discharged through the cavity orifice into the flow in micro passage. Determined by diaphragm amplitude, sufficiently strong jet momentum enables the jet to penetrate the micro passage flow to reach the heated (upper) wall within the time up to t = ½T at the peak diaphragm displacement.

In the figures, the formation of synthetic jet vortices is clearly visible during this initial phase of sequence. The flow patterns exhibits symmetry in Figure 4 (a) while the cross-flow drag imparted by the micro passage fluid stream gives rise to asymmetry in Figure 4 (b) where the jet is swayed in the streamwise direction.

For t > ½T, the diaphragm retreats from its peak displacement to complete the cycle. During this final phase, the synthetic jet mechanism draws fluid back into the cavity. Meanwhile, the synthetic jet vortices formed previously are dragged downstream by the micro passage flow.

As illustrated, the synthetic jet action periodically interrupts and breaks up the developing thermal and hydrodynamic boundary layers at the heated top wall of the micro passage. This flow interaction creates steep velocity and temperature gradients at the heated surface as long as jet impingement occurs. The pulsating jet flow mechanism therefore leads to improved thermal characteristics in the synthetic jet-mounted micro passage arrangement.

Effect of diaphragm amplitude

Relative strengths of the synthetic jet and the micro passage flow drag determine the extent of cross-flow interference and the boundary layer disruption at the heated wall. Comparison of velocity contours in Figure 5 (a) and (b) illustrates this effect on the jet behaviour. It is clearly seen that the increased micro passage flow impedes the jet impingement on the heated surface. Thus, the heat transfer rates will reduce with increased micro passage flow velocity. However, increasing the diaphragm amplitude will produce higher jet velocities permitting the jet to reach the heated wall for improved heat transfer rates.

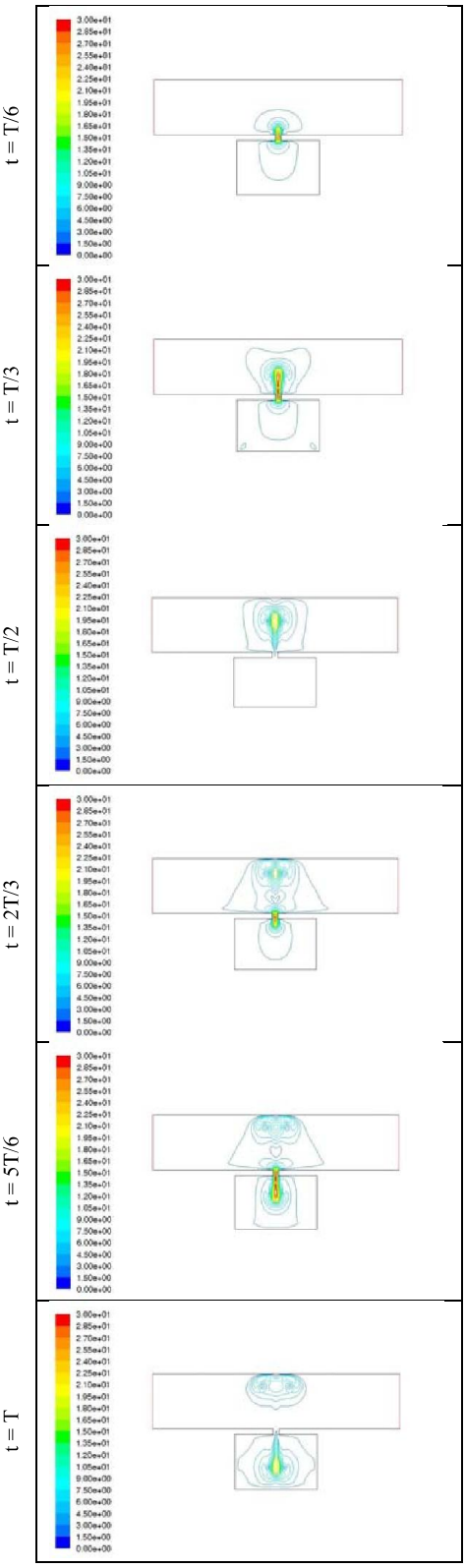

Figure 4 (a). Time-lapsed velocity contours over one diaphragm cycle
Micro passage velocity V_i = 0 m/s
A = 50 µm and f = 10 kHz

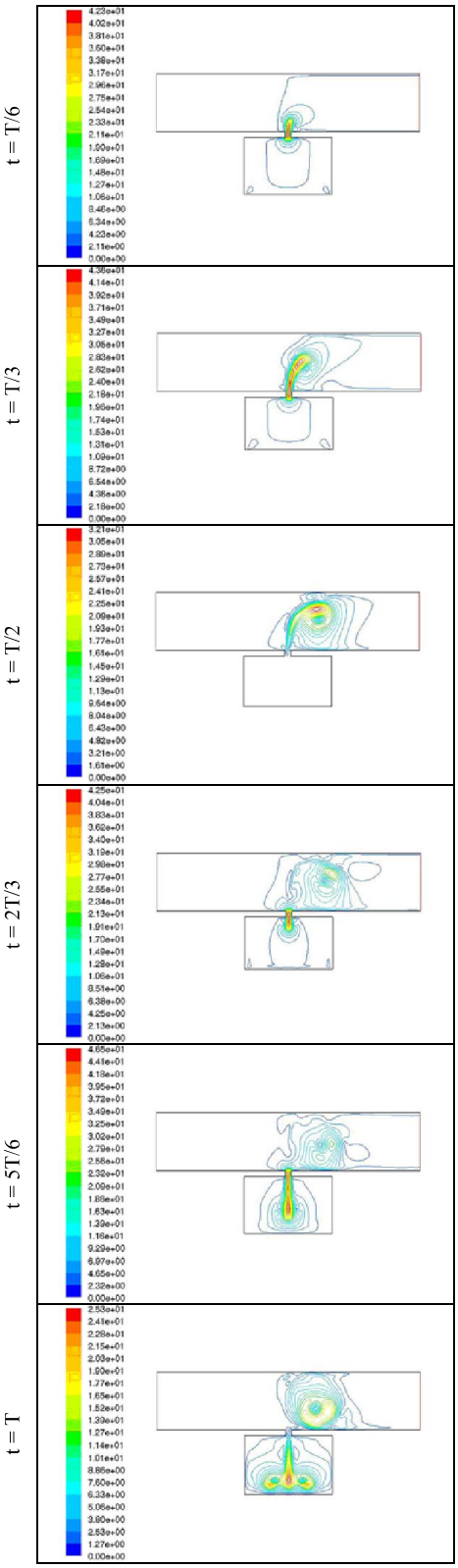

Figure 4 (b). Time-lapsed velocity contours over one diaphragm cycle
Micro passage velocity V_i = 0.5 m/s
A = 50 µm and f = 10 kHz

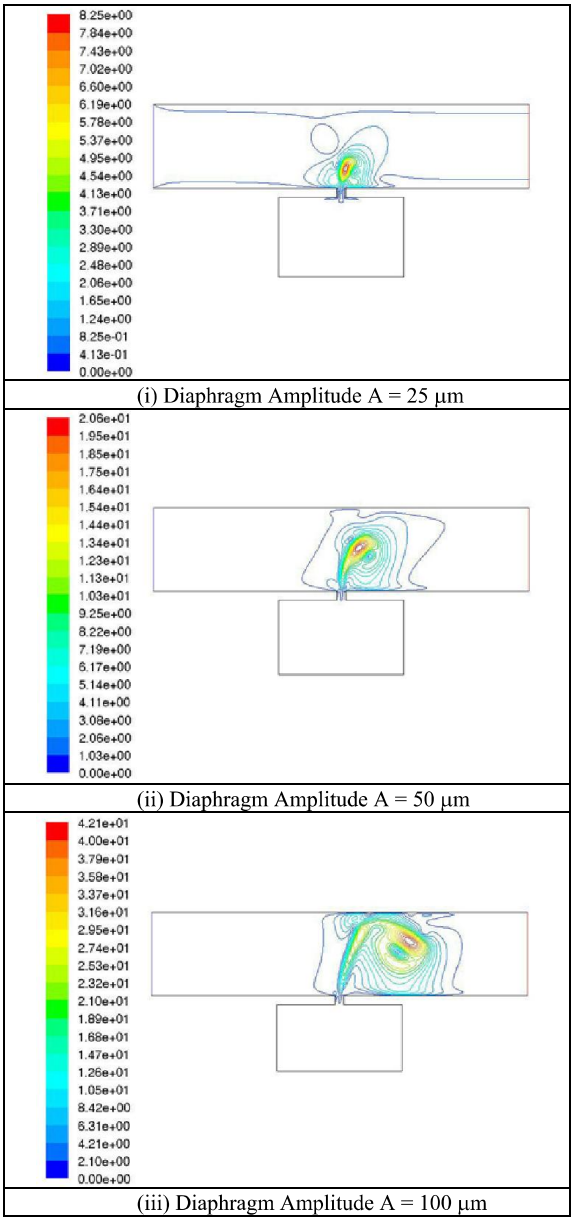

Figure 5(a). Velocity contours at t = ½ T
Micro passage inlet velocity V_i = 0.5 m/s
f = 10 kHz

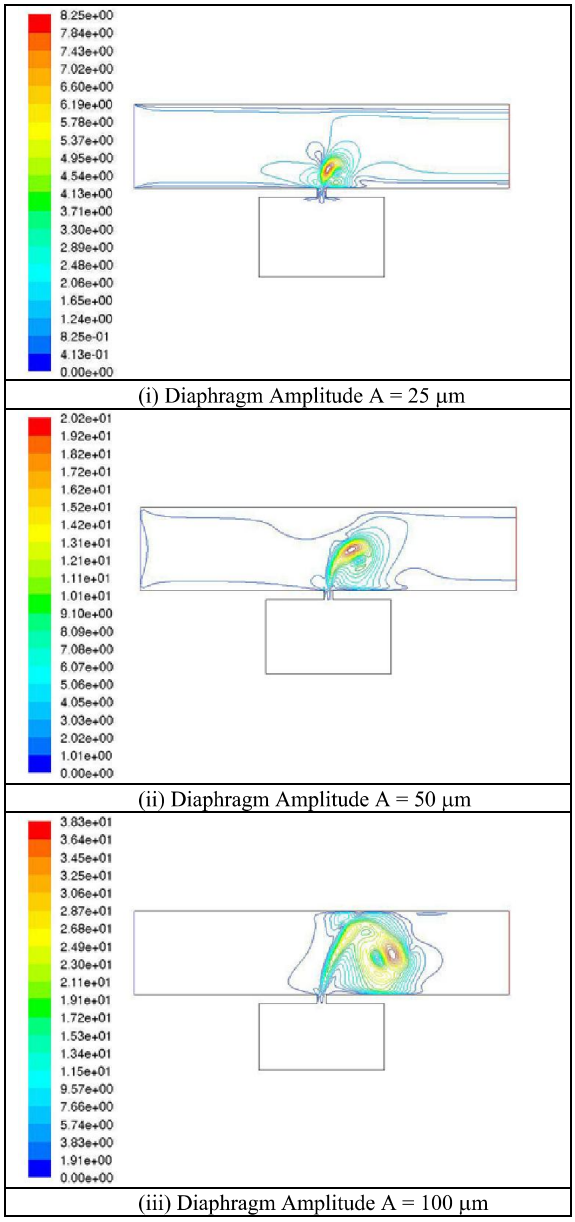

Figure 5(b). Velocity contours at t = ½ T
Micro passage inlet velocity V_i = 1.0 m/s
f = 10 kHz

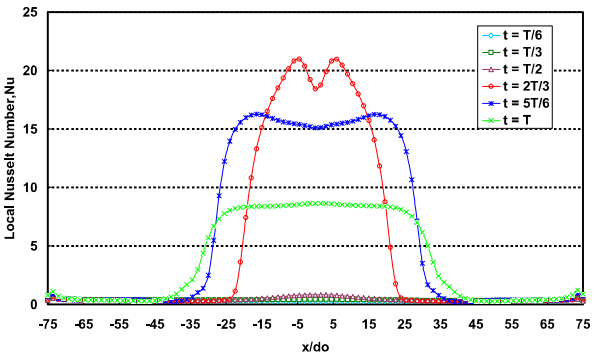

Figure 6. Distribution of local Nusselt number at the heated wall over one cycle
f = 10 kHz, A = 50 μm and V_i =0 m/s

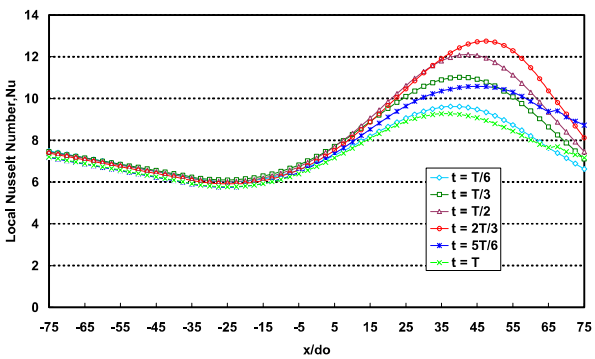

Figure 7. Distribution of local Nusselt number at the heated wall over one cycle
f = 10 kHz, A = 50 μm and V_i =1 m/s

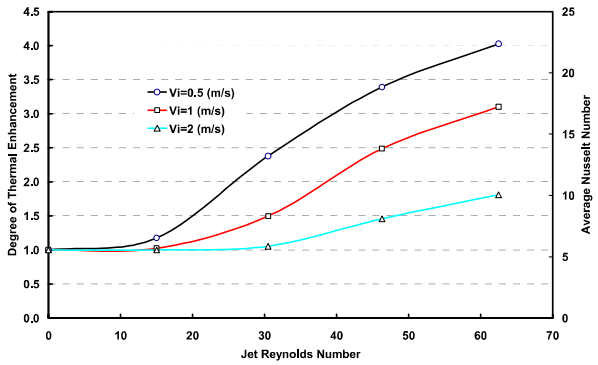

Figure 8. Degree of thermal enhancement and Nusselt number with synthetic jet mechanism

Heat transfer characteristics

For a typical case with stagnant fluid in the micro passage, Figure 6 shows the distribution of local Nusselt numbers over the heated wall for several time steps during one cycle of operation. It indicates that initially, the Nusselt number remains very low for $0 < t < \frac{1}{2}T$. During this period, the synthetic jet vortices have yet to impinge on the heated surface, as depicted in Figure 4(a). Therefore, the Nusselt number is essentially similar in magnitude to that of pure natural convection, which was estimated by a separate analysis to be about 0.2. The Nusselt number very rapidly increases to about 23 for $t = 2T/3$ when the vortices begin to interact with the heated surface, as shown in Figure 4(a). A gentle decline in the Nusselt number is then noticed for $t > 2T/3$. Thus compared to pure natural convection, the hybrid arrangement delivers over its operating cycle up to 120 times thermal enhancement at the heated wall.

Figure 7 shows a typical distribution of local Nusselt numbers at the heated wall over one cycle for the case of fluid flowing in the micro passage. It is noticed that the distribution now shifted downstream and the peak value of the Nusselt number is reduced to about 13. This is because the increased micro passage flow interacts with the impinging jet and drags it with the flow, as depicted in Figures. 4(b) and 5(a, b). Thus, the velocity and temperature gradients at the heated wall are reduced along with the heat transfer rates.

Thermal enhancement potential

Figure 8 shows the possible degree of thermal enhancement in the micro passage due to the periodic flow interaction induced by the synthetic jet mechanism. To be used as the datum, the performance of micro passage flow with no synthetic jet mechanism was estimated by a separate analysis. The enhancement value of 1 at zero jet Reynolds number represents this datum in Figure 8. For the tested range of diaphragm amplitude, jet frequency and micro passage velocity, the synthetic jet mechanism delivers the highest thermal enhancement of about 4.3 in the micro passage compared to a channel without pulsating jet. This clearly highlights the excellent thermal enhancement potential with this hybrid arrangement. The synthetic jet arrangement is able to achieve these excellent thermal characteristics without additional fluid circuits or increased micro passage flow rate or incurring extra pressure drop. To deliver this level of thermal performance without pulsed jet, the micro passage flow velocity would have to be raised by about 40 times yielding 70 fold increase in channel pressure drop as shown in Figure 9.

Figure 8 further shows that the higher micro passage velocity (cross-flow velocity) impairs thermal enhancement level. As explained previously with reference to Figure 5(a) and (b), the reason for this reduced thermal performance is due to the micro passage flow drag swaying the synthetic jet downstream preventing jet impingement on the heated surface. As the jet Reynolds number (or jet velocity or diaphragm amplitude) is increased for a fixed micro passage velocity, the degree of thermal enhancement suddenly increases when the jet is able to penetrate and reach the heated surface. A typical case for this is illustrated by the flow pattern depicted in diagram (ii) in Figure 5(a) for a micro passage velocity of 0.5 m/s. In Figure 8, the corresponding situation is shown by the onset of sudden elevation in thermal enhancement gradient at a jet Reynolds number of approximately 15. This point of rapid growth tends to shift towards higher values of jet Reynolds numbers as the micro passage cross-flow velocity is increased.

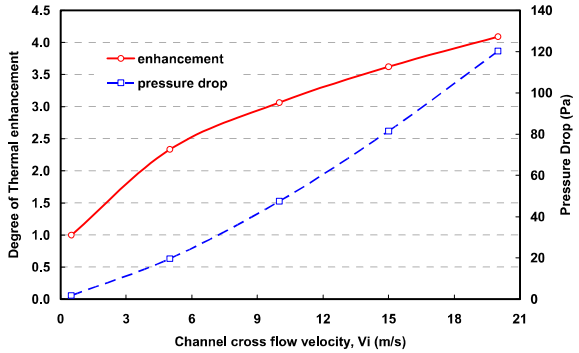

Figure 9. Degree of thermal enhancement and Nusselt number without synthetic jet mechanism

Compressibility effects on synthetic jet operation

Depending on the operating pressure range, the compressibility of the working fluid (air) could affect the behaviour of synthetic jet, particularly if the diaphragm undergoes high frequency oscillations. The present model examines such influences by performing identical simulations, first assuming constant air density and then considering density change with local pressure in the solution domain.

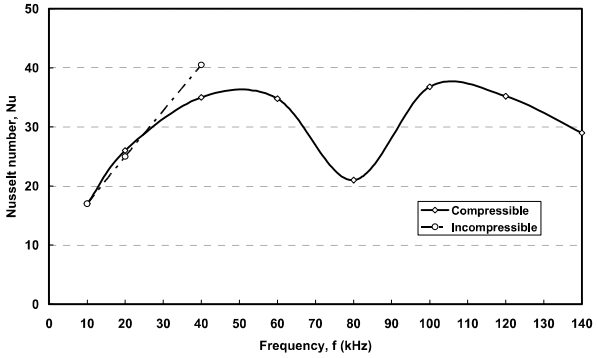

Figure 10. Effect of compressibility on the heat transfer characteristic

Figure 10 shows the variation of Nusselt number against diaphragm frequency with and without air compressibility in the analysis. The Nusselt number for both cases is seen to overlap each other and increase almost linearly for up to about 20 kHz. Around this value, the Nusselt number with compressibility indicates a sudden departure from that for incompressible case. The former shows a falling reduction in the magnitude while the latter continues to grow linearly.

Figure 10 further shows a dip in the Nusselt number at the diaphragm frequency of around 80 kHz. The computation indicates that at this operating frequency, the fluid discharge through the orifice is almost ceased and the entire pressure fluctuation is confined to the cavity volume. This is attributed to the opposing flow mechanisms within the cavity where the simultaneous expulsion and ingestion of air neutralising the flow though the orifice. Therefore, this frequency presents an interim limit on the synthetic jet operation beyond which it resumes functioning with its high effectiveness.

CONCLUSIONS

Through a numerical simulation, a novel thermal enhancement strategy for micro passages has been successfully demonstrated. The proposed technique incorporates a pulsating fluid jet generated by a special mechanism called "Synthetic Jet" that injects net positive fluid momentum with zero averaged jet mass flow into the micro passage. The pulsing jet interaction gives rise to excellent thermal characteristics at the heated wall when the fluid in the micro passage is stagnant as well as flowing. In the tested range, this unique technique is able to deliver up to 120 times heat transfer rates compared to pure natural convection at the heated wall and provides up to 4.3 fold enhancement in micro passage flow heat transfer. This excellent thermal performance is maintained over the entire tested frequency range except at a narrow high frequency band where the synthetic jet formation is subdued for fluid compressibility. The synthetic jet module examined achieves this excellent thermal performance without the deployment of additional fluid flow circuits or incurring extra pressure drop, which are adverse operational attributes of other common thermal enhancement strategies. This is recognised as the key operational attribute in this method that sets it apart from other thermal enhancement strategies. Along with these advantages, the improved thermal effectiveness of synthetic jets is highly justified for electronic cooling applications where intense localised cooling needs are desired.

REFERENCES

[1] Palm B. *Heat Transfer in Microchannels*. Microscale Thermophysical Engineering, 5(2001), pp. 133-175.

[2] Lee P.S and Garimella S.V and Liu D. *Investigation of Heat Transfer in Rectangular Microchannels*. International Journal of Heat and Mass Transfer, 48 (2005), pp. 1688-1704.

[3] Qu W and Mudawar I. *Experimental and Numerical Study of Pressure Drop and Heat Transfer in a Single Phase Microchannel Heat Sink*. International Journal of Heat and Mass Transfer, 45 (2002), pp. 2549-2565.

[4] Lee P.S and Garimella S.V. *Thermally Developing Flow and Heat Transfer in Rectangular Mircochannels*. International Journal of Heat and Mass Transfer, 49 (2006), pp. 3060-3067.

[5] Fedorov, A.G and Viskanta, R. 2000. "*Three Dimensional Conjugate Heat Transfer in the Microchannel Heat Sink for Electronic Packaging*". International Journal of Heat and Mass Transfer, **43**(3), pp. 399-415.

[6] Steinke M.E and Kandlikar S.G. *Single Phase Heat Transfer Enhancement Technique in Microchannel and Minichannel Flows*. Proceedings of International conference on Microchannel and Minichannels, pp.141-148. ICMM 2004-2328.

[7] Narayanaswamy R., Chandratilleke T.T and Foong J.L. *Laminar convective heat transfer in a microchannel with internal fins*. Proceedings of the 6th International ASME Conference on Nanochannels, Microchannels and Minichannels (ICNMM 2008-62044), Darmstadt, Germany.

[8] Campbell J.S, Black W.S, Glezer A and Hartley J.G.. *Thermal Management of a laptop Computer with Synthetic Air Microjets*. Proceedings of the IEEE InterSociety Conference on Thermal Phenomena, 1998, pp 43-50.

[9] Mahalingam R and Glezer A. *Air cooled heat sinks integrated with synthetic jets*. Proceedings of the IEEE InterSociety Conference on Thermal Phenomena, 2002, pp 285-291.

[10] Mahalingam R and Rumigny N. *Thermal Management using synthetic jet ejectors*. IEEE Journal, 27 (2004), pp 439-444.

[11] Holman R., Utturkar Y., Mittal R., Smith B.L and Cattafesta L. *Formation Criterion for synthetic jets*. AIAA Journal, 43 (2005), pp 2110-2116.

[12] Fugal S.R and Smith B.L. *A Numerical study of 2-D Synthetic jet formation*. Proceedings of ASME Heat Transfer/Fluids Engineering Summer conference, ASME, 2004, Charlotte USA.

[13] Wang Y., Yuan G and Bidstrup S.A. *Large eddy simulation (LES) for synthetic jet thermal management*. International Journal of Heat and Mass Transfer. 49 (2006), pp. 2173-2179.

[14] Chandratilleke T. T., Jagannatha D. and Narayanaswamy R. *Heat transfer enhancement in microchannels with cross-flow synthetic jets*. International Journal of Thermal Sciences, 49 (2010) pp 504–513

[15] FLUENT User Guide Manual 6.2.16, 2004.

[16] Smith B.L and Glezer A. *The Formation and evolution of synthetic jets*. Physics of fluids Journal, 10 (1998), pp 2281-2297.